TOXICOLOGICAL SCIENCES **124(2)**, 472–486 (2011)
doi:10.1093/toxsci/kfr233
Advance Access publication September 13, 2011

Susceptibility to Inhaled Flame-Generated Ultrafine Soot in Neonatal and Adult Rat Lungs

Jackie K. W. Chan,* Michelle V. Fanucchi,† Donald S. Anderson,* Aamir D. Abid,‡ Christopher D. Wallis,§ Dale A. Dickinson,† Benjamin M. Kumfer,‡,¶ Ian M. Kennedy,‡ Anthony S. Wexler,§ and Laura S. Van Winkle*,§,||,[1]

*Center for Health and the Environment, University of California, Davis, Davis, California 95616; †Department of Environmental Health Sciences, School of Public Health, University of Alabama at Birmingham, Birmingham, Alabama 35294-0022; ‡Department of Mechanical and Aerospace Engineering and §Air Quality Research Center, University of California, Davis, Davis, California 95616; ¶Department of Energy, Environmental and Chemical Engineering, Washington University in St Louis, Saint Louis, Missouri 63130; and ||Department of Anatomy, Physiology and Cell Biology, School of Veterinary Medicine, University of California, Davis, Davis, California 95616

[1]To whom correspondence should be addressed at Department of Anatomy, Physiology and Cell Biology, School of Veterinary Medicine, University of California, Davis, Davis, CA 95616-8732. Fax: (530) 752-7690. E-mail: lsvanwinkle@ucdavis.edu.

Received June 23, 2011; accepted August 24, 2011

Over a quarter of the U.S. population is exposed to harmful levels of airborne particulate matter (PM) pollution, which has been linked to development and exacerbation of respiratory diseases leading to morbidity and mortality, especially in susceptible populations. Young children are especially susceptible to PM and can experience altered anatomic, physiologic, and biological responses. Current studies of ambient PM are confounded by the complex mixture of soot, metals, allergens, and organics present in the complex mixture as well as seasonal and temporal variance. We have developed a laboratory-based PM devoid of metals and allergens that can be replicated to study health effects of specific PM components in animal models. We exposed 7-day-old postnatal and adult rats to a single 6-h exposure of fuel-rich ultrafine premixed flame particles (PFPs) or filtered air. These particles are high in polycyclic aromatic hydrocarbons content. Pulmonary cytotoxicity, gene, and protein expression were evaluated at 2 and 24 h postexposure. Neonates were more susceptible to PFP, exhibiting increased lactate dehydrogenase activity in bronchoalveolar lavage fluid and ethidium homodimer-1 cellular staining in the lung *in situ* as an index of cytotoxicity. Basal gene expression between neonates and adults differed for a significant number of antioxidant, oxidative stress, and proliferation genes and was further altered by PFP exposure. PFP diminishes proliferation marker PCNA gene and protein expression in neonates but not adults. We conclude that neonates have an impaired ability to respond to environmental exposures that increases lung cytotoxicity and results in enhanced susceptibility to PFP, which may lead to abnormal airway growth.

Key Words: **lung development; polycyclic aromatic hydrocarbons; antioxidants; oxidative stress.**

Airborne particulate matter (PM) pollution is an aggregate mixture of small particles and liquid droplets present in the atmosphere as defined by the EPA. Fine particles ($PM_{2.5}$; aerodynamic diameter < 2.5 μm) are highly prevalent. It is estimated that over 28% of the U.S. population live in areas exceeding EPA standards (USEPA, 2009). Exposure to fine particles has been linked to development of respiratory infections, exacerbation of asthma, and increased risk of respiratory and cardiovascular morbidity and mortality, especially in susceptible populations (ALA, 2009; Dockery, 2009; Mills *et al.*, 2009). Although exposure to ultrafine particles ($PM_{0.1}$; aerodynamic diameter < 0.1 μm) has also been linked to diminished lung development and function (Ibald-Mulli *et al.*, 2002), exposure levels are currently unregulated.

Young children are especially susceptible to PM. They are more aerobically active outdoors, have a larger body surface area-to-volume ratio, higher metabolic rate, have higher minute ventilation, and increased oxygen consumption per body weight compared with adults (Bearer, 1995). Their small body size, smaller mean airway diameter with increased air exchange exacerbates particle deposition (Branis *et al.*, 2009). Furthermore, lungs continue to grow and mature postnatally and are exposed to PM during this period of maturation (Langston, 1983). Susceptibly may be altered due to the extensive and continuous growth, differentiation, and maturation of the bronchiolar airways and alveoli. Acute exposures to PM have been associated with an increased incidence of respiratory hospital admissions and medication use in asthmatic children (Pekkanen *et al.*, 1997; Peters *et al.*, 1997; Norris *et al.*, 1999). Children living in areas of high levels of short-term particulate pollution (i.e., near roadways) have increased morbidity and mortality from respiratory illnesses, such as bronchitis and pneumonia in a dose-dependent manner (Ciccone *et al.*, 1998). It is clear from the epidemiologic data that PM exposures affect the incidence and severity of lung diseases in children, diseases of airways in particular. Despite a large body of epidemiologic data correlating adverse health effects from PM exposure, biochemical mechanisms of toxicity in the developing lung remain

relatively unexplored. This may be due to the complicated spatiotemporal variation in PM containing atmospheres as well as the dauntingly complex mixture of PM and gases that characterize these atmospheres. Sampling sites, seasonal variations, and time of day all play a role in defining particle composition. This complicates the systematic study of health effects. Despite this, it is well established that vehicular exhaust from combustion of gasoline, diesel, and other petroleum fuels is the dominant contributor to the fine and ultrafine particulate ranges (Pey *et al.*, 2009). Combustion in vehicle engines may be incomplete and lead to the emission into the atmosphere of carbonaceous particles and a variety of fused and free polycyclic aromatic hydrocarbons (PAHs). Due to the highly variable nature of outdoor ambient PM, we have developed and used a premixed flame particle (PFP) generating system (Lee *et al.*, 2010) to create an exposure atmosphere for *in vivo* studies. PFPs are generated in a laminar fuel-rich flame resulting in fine and ultrafine particles. A variety of PAH species are present in both the particulate and vapor phases. PFP is used as a surrogate for toxicity testing of combustion-generated aerosols and associated PAH. This allows for modifications of PM composition (i.e., PAH content, metals, gases, etc.) in addition to the ability to reproducibly generate similar environments without potential confounders like temperature, weather, variations in air quality, allergens, or metals present in field samples.

In the current study, we characterized the PFP environment as well as acute exposure responses in 7-day-old postnatal and young adult rats following *in vivo* exposure to either PFP or filtered air (FA). We hypothesized that neonates would have altered oxidative stress and antioxidant expression patterns resulting in increased cytotoxicity and susceptibility to PFP. The objectives of this study are: (1) to characterize the PFP environment and quantify free and fused PAH content within the chamber atmosphere, (2) to define PFP cytotoxicity and susceptibility in neonates and adults, and (3) to determine whether the airway oxidative stress gene response varies by age.

MATERIALS AND METHODS

Flame and particle characterization. PFPs were generated using a coannular premixed flame burner (Fig. 1A). The burner consists of a 7.1-mm tube (inner diameter) surrounded by an 88.9-mm concentric outer tube (inner diameter). The burner is enclosed in a Pyrex tube to isolate the burner from ambient air. A mixture of ethylene, oxygen, and argon was metered through the inner tube at 212.4 cc/min, 289.2 cc/min, and 1499 cc/min, respectively, using mass flow controllers (model 647C flow control unit and model 1179A and M100B flow control valves, MKS Instruments, Andover, MA). A small flow rate of oxygen (52 cc/min) flowed through the outer annulus to stabilize the flame. The flame was shielded from room air by a curtain flow of nitrogen metered at 10 l/min using a Fisher and Porter variable area flow meter (Andrews Glass, Vineland, NJ) and delivered around the circumference of the burner chamber. Filtered dried air was added to the flow downstream of the flame, and all burner effluent passes through a heated 3-way catalyst to remove NO_x and CO. PFP were diluted with clean HEPA and CBR (chemical/biological/radiological) FA and mixed into a mixing chamber before entering the inhalation exposure chamber (Fig. 1B).

Animals underwent a whole-body exposure to the flame-generated particles. Chamber CO levels were monitored using a Teledyne-API Model 300E CO analyzer (San Diego, CA) and was calibrated with an NIST traceable span gas of 202.4 ppm CO diluted in ultrapure air to 10 ppm CO for calibration (Scott-Marrin Inc., Riverside, CA). Chamber NO_x levels were monitored (Dasibi 2108 Chemiluminescence NO_x Analyzer, Glendale, CA). PFP was collected directly from the exposure chamber for analysis though ports in the chamber wall. Particle number concentration was determined using a condensation particle counter (CPC, TSI model 3775, Shoreview, MN). Particle size distribution was determined using a scanning mobility particle sizer (SMPS) (model 3080 electrostatic classifier with model 3081 differential mobility analyzer) and a model 3020 CPC (TSI).

PFP mass concentration was determined by collecting particles from the chamber on glass fiber filters (Pallflex Emfab 47-mm filters, Ann Arbor, MI) placed in a filter housing (BGI, Waltham, MA). The sampling flow rate was set at 20 l/min air flow rate driven by a vacuum source downstream of the flow.

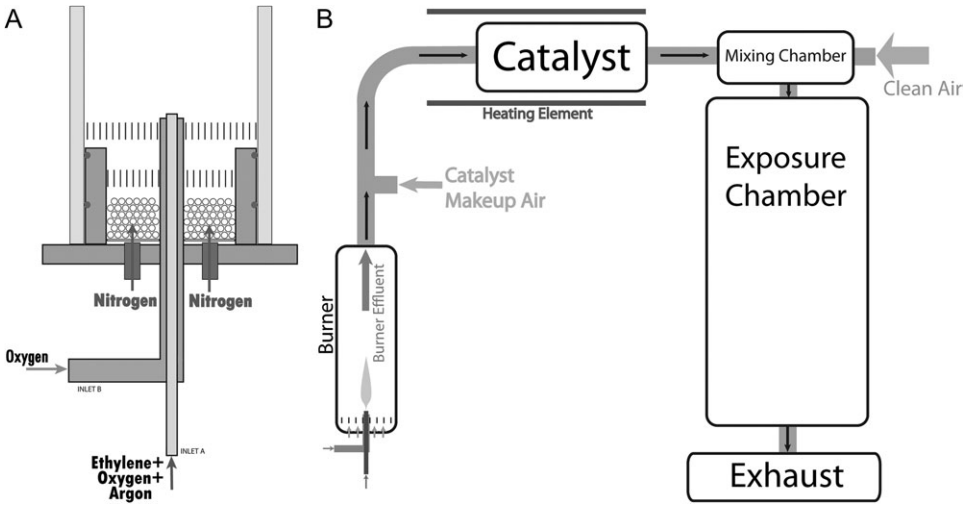

FIG. 1. Premixed flame burner and chamber schematic. (A) Premixed fuel and oxidized flow through the central annulus. The flame is stabilized by an outer annular oxygen flow. The flame is shielded from room air by an outer nitrogen coannular flow. (B) Particle laden gas is passed through a catalytic converter to remove NO_x and CO. The flow is diluted before entering the exposure chambers.

Collection was performed for the duration of the exposure. Total particulate mass was determined gravimetrically (Sartorius AG MC5 microbalance, Goettingen, Germany). Particle samples were collected on 47-mm glass fiber filters (Pallflex Tissuequartz, Ann Arbor, MI) for elemental carbon to organic carbon ratio (EC/OC) analysis as described above. The EC/OC ratio was determined using a method previously described (Herner *et al.*, 2005; Robert *et al.*, 2007). Particle and vapor phase PAH speciation was performed by the Desert Research Institute (DRI, Reno, NV). PFP were collected on Pallflex Tissuequartz 47-mm filters, and vapor phase organic compounds were collected on XAD resin supplied by DRI.

Transmission electron microscopy. PFP were sampled via an electrostatic precipitator (ESP) similar in design to that described previously (Morrow and Mercer, 1964). Particles were sampled from the exposure chamber using $^1/_4$ " inch conductive tubing and drawn through the ESP using a vacuum pump. The sampling flow rate was 100 cm^3/min, and the ion current was set to 3.5 μA. The morphology of soot particles were analyzed by transmission electron microscopy (Phillips CM-12, LaB_6 cathode, operated at 120 kV), and carbon coated copper grids were used for particle sampling (300 mesh, lacey carbon type-A substrate, Ted Pella Inc. Redding, CA).

Animals and exposure protocol. Two and a half month reproductively capable young adults approximating peak fitness and newborn postnatal male Sprague Dawley rats with accompanying dams were obtained from Harlan Laboratories and allowed to acclimate in CBR FA exposure chambers until newborn pups reached 7 days of age in a 12 h light/dark cycle. Animals were acutely exposed in a whole-body chamber to either 6 h of FA or an atmosphere of 22.40 ± 5.60 μg/m^3 PFP (mean ± SD). Two identical custom-built exposure chambers were used for the exposure experiments, one chamber housed PFP-exposed animals and the other housed age matched FA control animals (Hinners *et al.*, 1968). The stainless steel chambers have a volume of 3.8 m^3. A mixing chamber located at the top of the animal chamber where CBR filtered room air was mixed with PFP. Chambers were maintained at −0.3 inches of H_2O gage pressure, and temperature were maintained between 22.2°C and 24.4°C. The FA flow rate through the chamber was set at 30 air exchanges per hour. During exposure, adult rats were housed in stainless steel wire cages. Due to size differences, 7-day-old postnatal rats were housed with lactating females in polycarbonate cages with wire lids during exposure; Kimwipes (Kimberly-Clark, Neenah, WI) were used for bedding during the exposure period. Cages were arranged in the chamber in a single level and were cleaned with bedding changed every other day. Adult rats were provided with Laboratory Rodent Diet (Purina Mills, St Louis, MO) and water *ad libitum*. All animal experiments were performed under protocols approved by the University of California Davis IACUC in accordance with National Institutes of Health guidelines. Animals were necropsied 2 or 24 h following cessation of the 6-h exposure. All animals were euthanized through ip injection of an overdose of pentobarbital (150 mg/kg). At necropsy, tracheas were cannulated, the thorax was opened, and lung removed en bloc for processing.

Ethidium homodimer-1 cell viability assay. Rat lungs were examined for the presence of membrane permeable cells as previously described (Van Winkle *et al.*, 1999). Two hours after exposure, rat lungs were intratracheally inflated with 10μM Ethidium Homodimer-1 (Molecular Probes, Carlsbad, CA) in warmed F-12 media (Gibco, Carlsbad, CA) for 15 min. Ethidium Homodimer-1 containing media was removed, and lungs were rinsed three times with warmed F-12 media to remove unbound dye. Lungs were fixed in Karnovsky's fixative (Karnovsky, 1965) under 30-cm hydrostatic pressure for 1 h and stored at 4°C until paraffin embedment. Sections were analyzed using epifluorescent microscopy and subsequently counterstained with Hematoxylin and Eosin (H & E) for cellular identification.

Lactate dehydrogenase cytotoxicity and total protein assays. Bronchoalveolar lavage fluid (BALF) was collected through recovery of intratracheal instillation of Hank's Buffered Salt Solution (Gibco, Carlsbad, CA) at 35 μl/g body weight concentration to scale for differences in animal size. Lactate dehydrogenase (LDH) activity (U, the amount of LDH that catalyzes the reaction of 1 μmol of substrate per minute) in BALF was detected using an LDH Cytotoxicity Assay Kit (Cayman Chemical Company, Ann Arbor, MI) following manufacturer instructions. LDH activity was determined to have a detection limit of 0.16 U/ml BALF from serial dilutions of an LDH standard. BALF protein concentrations were determined using the Micro Lowry Total Protein Kit (Sigma Chemical, St Louis, MO).

RT-profiler arrays on microdissected airways. Lungs were filled to capacity with and preserved in RNAlater (Ambion, Austin, TX) at −20°C until microdissection. RNA later stabilized intrapulmonary airways from the lobar bronchus to the terminal bronchioles were dissected free from the surrounding parenchyma as described in Baker *et al.* (2004). Airway enriched RNA (362–1185 ng/μl RNA; 18.1–59.25 μg RNA per animal) was isolated using Tri Reagent (Molecular Research Center, Inc., Cincinnati, OH) following the manufacturer's protocol based on the method detailed in Chomczynski and Sacchi (1987). RNA purity was confirmed through spectrophotometric absorbance at 260/280 nm. cDNA was synthesized and amplified using the RT^2 PreAMP cDNA Synthesis Kit (SABiosciences, Frederick, MD). RT amplification data for all samples reported "pass" for all internal reverse transcription efficiency and genomic DNA contamination quality controls prior to analysis. Relative quantification of gene expression for each sample was performed on airways from each animal individually using quantitative RT-PCR on RT^2 qPCR Arrays (cat# PARN-003, PARN-065) strictly following manufacturer's instructions (SABiosciences). A complete list of genes assayed is available (Supplementary tables 1S–3S). Results were calculated following the RT^2 Profiler PCR Array Data Analysis tool, available online at http://pcrdataanalysis.sabiosciences.com/pcr/arrayanalysis.php (SABiosciences). Differential gene expression data across age and treatment groups were analyzed using hypoxanthine-guanine phosphoribosyltransferase (HPRT) as the reference gene. HPRT was chosen as the reference gene due to consistency and low variance between exposures and within age groups as assessed previously (Van Winkle *et al.*, 2010). Gene expression heatmap was generated using the RT^2 Profiler PCR Array Data Analysis tool, with each lane representing the averaged fold change from multiple animals within each group for each significantly changed gene, either by age and/or exposure. Results are expressed as a fold change in gene expression relative to FA animals of the same age, unless otherwise stated. The number of animals assessed per exposure group using the RT^2 qPCR Arrays was: 7-day-old FA (3), 7-day-old PFP exposed (3), Adult FA (3), and Adult PFP exposed (6).

Proliferating cell nuclear antigen immunohistochemistry. Lung tissue prepared for immunohistochemical analysis was inflated with 37% formaldehyde vapor bubbled under 30-cm hydrostatic pressure for 1 h as previously described (Hammond and Mobbs, 1984; Wilson *et al.*, 2001). Samples were stored in 1% paraformaldehyde for less than 24 h prior to processing and paraffin embedment. Paraffin sections were immunostained using methods previously described (Van Winkle *et al.*, 1996). Briefly, slides were boiled in hot citrate buffer for antigen retrieval. Endogenous peroxidase activity was quenched with a 10% hydrogen peroxide solution, and nonspecific binding was blocked with IgG-free bovine serum albumin (Jackson ImmunoResearch Laboratories, West Grove, PA) for 30 min. Sections were immunostained against proliferating cell nuclear antigen (PCNA) using a monoclonal anti-PCNA antibody (DAKO, Carpinteria, CA) at dilution of 1:600 overnight at 4°C (Van Winkle *et al.*, 2010). Signal was visualized using the avidin-biotin-peroxidase ABC kit (Vector Labs, Burlingame CA) and 3,3′-diaminobenzidine tetrahydrochloride (Sigma Chemical) as the chromagen. Sections from all groups were stained simultaneously to minimize variability in between runs. Controls included substitution of primary antibody with phosphate buffered saline and testing all antibodies in a series of dilutions prior to use to optimize staining.

Statistics. All data are reported as mean ± SEM unless otherwise stated. Statistical outliers in PFP chamber mass concentration were eliminated using the extreme studentized deviate method (Graphpad, La Jolla, CA). LDH data containing samples below detection limit (BDL) were treated as nondetected

(NDs), and values were imputed using the natural-log regression on order statistics (lnROS) method (Helsel, 2005; Shumway *et al.*, 2002) using ProUCL (U.S. EPA, Atlanta, GA). Two-way ANOVA was applied against age and exposure factors when appropriate. Multiple comparisons for factors containing more than two levels were performed using Fisher's Protected Least Significant Difference (PLSD) method. Pair-wise comparisons were performed individually using a one-way ANOVA followed by PLSD post hoc analysis using StatView (SAS, Cary, NC). For RT-profiler array data, statistical functions were performed using the online RT^2 Profiler PCR Array Data Analysis tool (SABiosciences), where p values are calculated based on a Student's t-test of the replicate $2^{-\Delta\Delta Ct}$ values for each gene in the control and treatment groups. p values of < 0.05 were considered statistically significant.

RESULTS

Characterization of Premixed Flame Generated Atmosphere

Rats were exposed for 6 h to a premixed flame generated atmosphere; dams were exposed with their pups. The atmosphere contained both particles and gases. Both were characterized (Fig. 2, Supplementary tables 1S and 2S), and the abundance reported is the average of two collections.

Using data from a series of PFP exposures, the exposure chamber mass concentration was determined to be 22.40 ± 5.60 $\mu g/m^3$ PFP (mean ± SD) based on gravimetric filter measurement. SMPS measurements showed a geometric mean mobility diameter of 70.56 nm with a geometric standard deviation of 1.51 nm. The mean particle number concentration was $9.37 \times 10^4 \pm 4.8 \times 10^3$ particles/cm^3 (mean ± SD) based on CPC measurements over duration of exposure. PFP exposure chamber CO levels were within 0.2 ppm of FA chamber levels, with quantification below 0.2 ppm limited by instrument accuracy. Chamber NO and NO_2 concentrations were within 0.01 ppm of FA levels. Particles were high in organic carbon and had an EC/OC ratio of 0.58. The amount of total PAH measured on PM was 54 ng/m^3 and the amount of gas phase PAH was 405 ng/m^3. The 20 most abundant vapor phase and particulate phase PAHs are listed (Tables 1 and 2). In general, biphenyls and naphthalene compounds dominated the vapor phase, and non, mono, and poly substituted naphthalenes constituted the particulate phase. Typical morphologies of PFP are shown (Figs. 2C–E) where soot particles are composed of 10–20 nm round primary particles forming larger fractal aggregates.

Cytotoxicity of PFPs

To evaluate airway epithelial membrane permeability after PFP inhalation, we compared *in situ* ethidium homodimer-1 fluorescence (red) overlaid upon tissue autofluorescence (green) as a marker for cytotoxicity in 7-day-old neonates and adults 2 h following either a single acute 6 h PFP exposure or FA using epifluorescence microscopy (Fig. 3). The airway epithelium between adult and neonates was similar among exposure groups. Ethidium homodimer-1 positive membrane permeable cells were rarely detected in either age group reared in a FA environment (Figs. 3A and 3D). However, 2 h following PFP exposure, membrane permeable cytotoxic cells

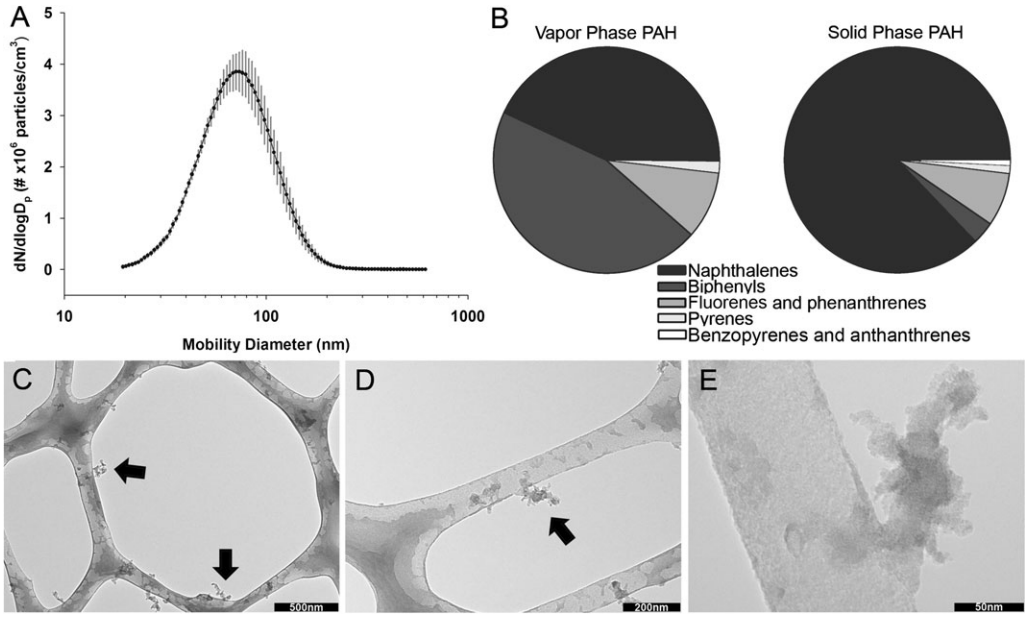

FIG. 2. PFP characterization. (A) Soot size distribution within exposure chamber indicates a geometric mean particle size of 70.56 ± 1.51 nm (geometric mean ± geometric SD). (B) Total amounts of PAH present were 405 ng/m^3 in the vapor phase and 56 ng/m^3 in the particulate phase. Low molecular weight aromatic hydrocarbons such as methylated biphenyls (182 ng/m^3), naphthalene (19 ng/m^3), mono, and poly methylated naphthalenes (149 ng/m^3) were major constituents in the vapor phase. In contrast, naphthalene (15 ng/m^3) and methylated naphthalenes (33 ng/m^3) dominated the solid particle phase. (C–E) Transmission electron micrographs of particle morphology sampled on a lacy carbon substrate indicate oily particles with primary particle sized between 10 and 20 nm forming larger fractal aggregates (arrows).

TABLE 1
Top 20 Most Abundant PAHs in Vapor Phase

Compound	Abundance (ng/m^3)
2-methylbiphenyl	114.68
3-methylbiphenyl	64.30
2-methylnaphthalene	35.86
1,3 + 1,6 + 1,7dimethylnaphth	23.78
Naphthalene	18.73
1-methylnaphthalene	17.51
2,6 + 2,7-dimethylnaphthalene	14.22
1 + 2ethylnaphthalene	12.61
Fluorene	11.54
C-trimethylnaphthalene	8.41
B-trimethylnaphthalene	7.72
2,3,5 + I-trimethylnaphthalene	7.42
Phenanthrene	6.65
1,4 + 1,5 + 2,3-dimethylnaphth	6.04
E-trimethylnaphthalene	4.97
F-trimethylnaphthalene	4.74
2-methylphenanthrene	4.28
4-methylbiphenyl	3.36
C-dimethylphenanthrene	2.98
Quinoline	2.60

were readily detected in the subepithelium and parenchyma near terminal bronchioles (Fig. 3E) in the neonates, while bronchiolar airways remained intact and viable (data not shown). High-magnification micrographs reveal the presence of ethidium positive macrophages after PFP exposure (Figs. 3F and 3G) that were absent in FA animals (Figs. 3B and 3C). Adult animals exhibited less susceptibility after PFP exposure. Membrane permeable cells were rarely observed, with the exception of a few sparse ethidium positive cells present in a few terminal bronchioles (Fig. 3H).

TABLE 2
Top 20 Most Abundant PAHs in Particulate Phase

Compound	Abundance (ng/m^3 air)
Naphthalene	15.37
2-methylnaphthalene	13.84
1-methylnaphthalene	6.57
1,3 + 1,6 + 1,7dimethylnaphth	5.89
2,6 + 2,7-dimethylnaphthalene	2.68
9-methylphenanthrene	1.91
1 + 2ethylnaphthalene	1.45
Biphenyl	0.76
1,4 + 1,5 + 2,3-dimethylnaphth	0.76
3-methylbiphenyl	0.76
Phenanthrene	0.46
C-trimethylnaphthalene	0.38
Quinoline	0.38
3-methylphenanthrene	0.31
4-methylbiphenyl	0.31
Fluorene	0.23
Retene	0.23
Acenaphthene	0.15
D-dimethylphenanthrene	0.15
Dibenz(a,h)acridine	0.15

To quantitatively measure cytotoxicity, we measured LDH activity and total protein present in BALF as a global marker of lung cell injury (Fig. 4). In all neonates exposed to FA, LDH activity was found to be indistinguishable from background levels of BALF, as determined by the detection limit of our assay (<0.16 U/ml BALF), which was used for statistical analysis. To discern whether age (neonates vs. adults) and/or exposure (FA vs. 2 or 24 h post PFP exposure) affects LDH activity (U) normalized to milliliters of BALF volume (Fig. 4A), we used a two-way ANOVA and found significant main effect of age ($p < 0.0001$), indicating that adults have greater LDH activity than neonates. There was also a main effect of exposure ($p = 0.0398$), showing a significant difference in LDH activity as a function of time after PFP exposure. Additionally, there was an interaction between age by exposure ($p = 0.0402$). To determine specific interactions among groups, a one-way ANOVA with Fisher's PLSD *post hoc* analysis revealed significantly higher basal levels in adults compared with neonates ($p < 0.0001$). A transient drop in LDH activity was seen in adult 2 h post PFP exposure ($p = 0.0024$). Contrary to adults, neonates trended upward after PFP exposure, reaching significance at 24 h post exposure compared with FA controls ($p = 0.0106$).

Next, we measured total protein levels in BALF (Fig. 4B). A significant main effect of age ($p < 0.0001$) showed that adults have more protein in BALF than neonates. Secondly, an interaction between age by exposure ($p = 0.0263$) was also significant. Pairwise comparisons reveal elevated basal levels of protein in control adults ($p = 0.0218$). While protein concentrations remained steady in either age groups 2 h post PFP exposure, total protein in BALF was significantly greater in adults 24 h after PFP, compared against FA controls ($p = 0.0424$).

Finally, two-way ANOVA analysis of LDH activity normalized to BALF protein (Fig. 4C) did not reveal differences between any main effects. However, a significant age by exposure interaction ($p = 0.0094$) was observed. Pairwise comparisons showed a significantly greater normalized LDH activity in adults ($p = 0.0083$). Additionally, a markedly amplified trend was seen in neonates, peaking at 24 h post PFP, where normalized LDH activity were significant compared against both FA controls ($p = 0.0019$) and 2 h following PFP ($p = 0.0056$).

PFP-Induced Antioxidant and Oxidative Stress Response

In an attempt to characterize the oxidative stress and antioxidant responses, we measured individual gene transcription in the conducting bronchiolar airways of neonatal and adult rats 24 h after the cessation of either PFP or FA exposure. We used the "Oxidative Stress and Antioxidant Defense" and "Stress and

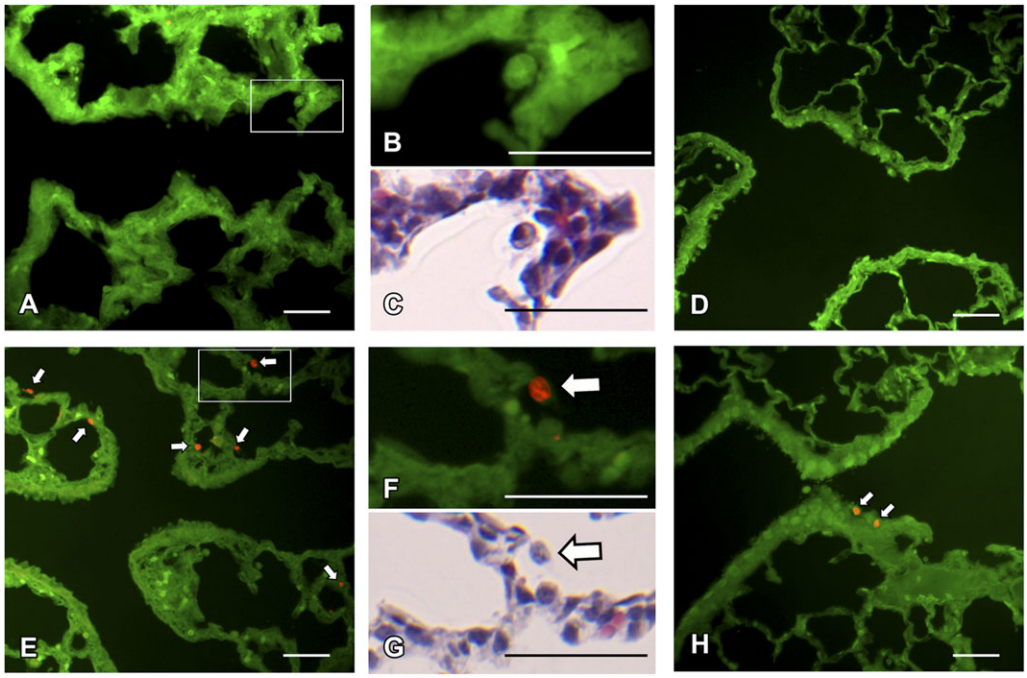

FIG. 3. Airway epithelial cellular toxicity following PFP exposure. *In situ* ethidium homodimer-1 sections were analyzed in 7-day postnatal (A, E) and adult rats (D, H) exposed to either FA (A–D) or PFP (E–H) for regional localization of membrane permeable cytotoxic cells. Overall, ethidium positive cells (red fluorescence) were scarcely observed in either 7-day old neonatal rats (A) or adults (D) reared in FA. Resident macrophages are depicted (B, C) to show a lack of ethidium uptake under FA conditions. However, 2 h following PFP exposure, membrane permeable cells (white arrows) were readily detected in the neonates in the subepithelium and parenchyma (E). A high magnification insert (F) and subsequent H & E stained section (G) shows that the majority of membrane permeable cells present are either monocytes or macrophages. In adults following PFP exposure, adult rat bronchiolar airways remained mostly noncytotoxic, with the exception of a few ethidium positive cells in the terminal bronchioles (D). Scale bars are 50 μm.

Toxicity Pathwayfinder" RT^2 RT-profiler qPCR arrays to quantify 162 genes using RNA extracted from microdissected airway trees. Overall, we saw very diverging trends in gene expression between neonates and adults. While a majority of the genes within the two array panels were upregulated in neonates, the opposite was observed in adults (Fig. 5A). Seventy-eight genes were determined to be differentially expressed either as function of age and/or exposure (Fig. 5B, Supplementary tables 1S–3S). First, we focused on genes that have been significantly altered due to PFP exposure. In neonates (Table 3), 24 genes were found to have significantly deviated from FA controls, with 11 of these genes categorized under "Antioxidant and Oxidative Stress" response and related genes. Specifically, many genes encoding enzymes with xenobiotic conjugation activities such as the glutathione and prostaglandin peroxidase families were upregulated after PFP exposure. Additionally, growth and senescence-related genes, like *PCNA*, were downregulated while cell checkpoints Cyclin C (*Ccnc*) and G1 (*Ccng1*) were upregulated in the young animals.

In contrast to neonates, adult rats had a more robust response, with 53 genes changed (Table 4). Although the majority of genes (25) altered fall under Antioxidant and Oxidative Stress response genes, only six genes (*Gpx1*, *Gstm1*, *Gstm3*, *Hmox2*, *Ptgs2*, and *Xpa*) significantly matched between the two ages. Furthermore, there was a dissimilar response in "Necrosis and Apoptosis" and "Proliferation and Carcinogenesis" categories compared against the different ages. While downregulation was primarily observed in adults, neonates had a more divergent response with some genes upregulated and some downregulated. Only Annexin A5 (*Anxa5*) matched as significantly changed among the two ages in these categories. Interestingly, we have also detected changes in xenobiotic metabolizing genes in the cytochrome P450 and Flavin moooxygenase families that were not observed in 7-day-old postnatal animals. To reduce the analysis from the large data set, we focused on a subset of genes that were either significantly altered in both 7-day-old postnatal and adult animals, and/or genes that we have analyzed previously in studies of other particle types (Lee *et al.*, 2010; Van Winkle *et al.*, 2010). These have been plotted as relative fold change as compared with age-matched FA controls (Fig. 5C).

PCNA Expression

PCNA, a gene associated with cell proliferation was quantified from RT-profiler array data from microdissected airways using the comparative Ct method with HPRT as the reference gene. PCNA expression in FA 7-day postnatal rats was about 5-fold higher than FA adults. Twenty-four hours following PFP exposure, PCNA expression was significantly reduced while expression remained unchanged in adults. To qualitatively determine protein abundance, immunohistochemical staining

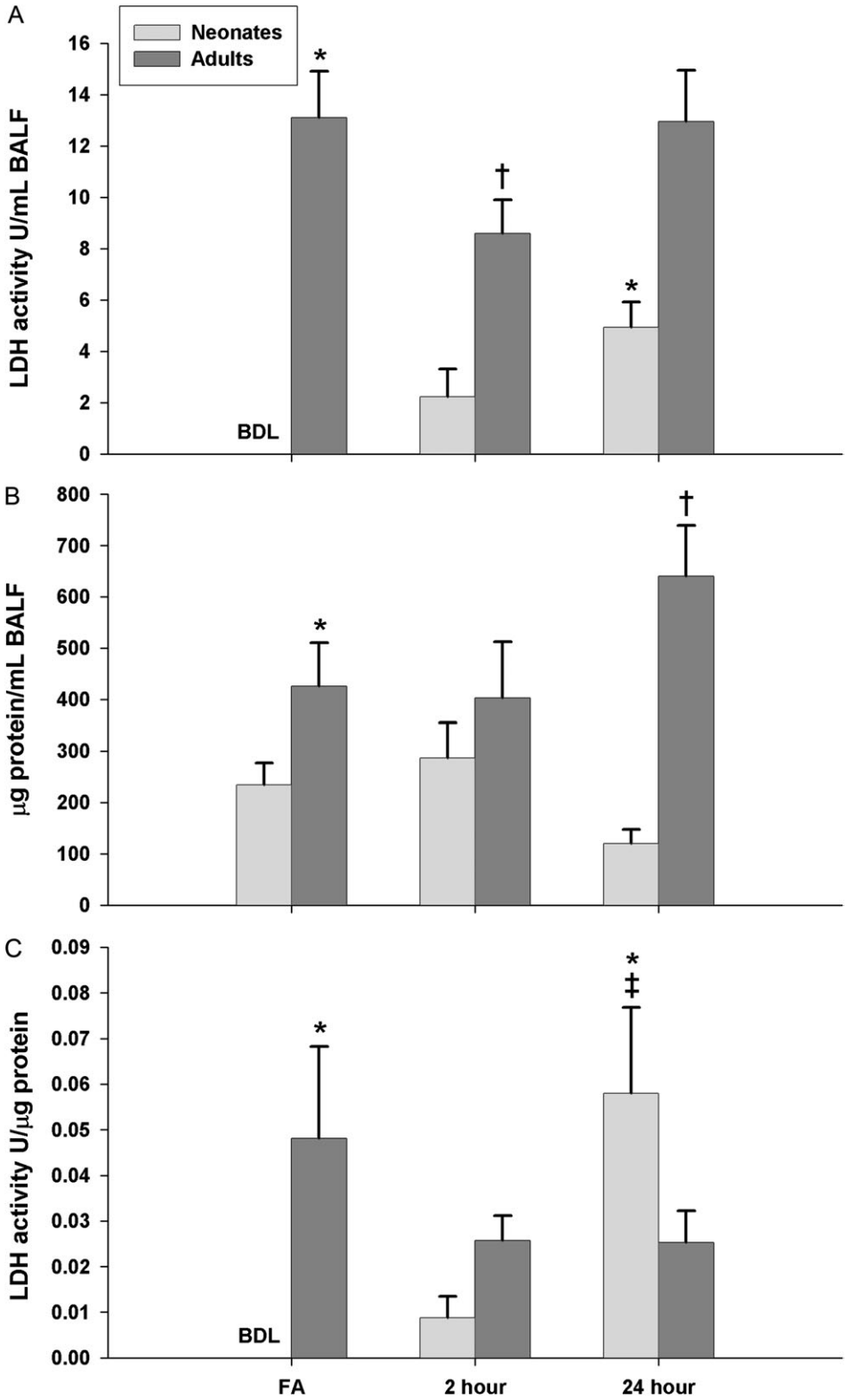

FIG. 4. Cellular permeability in BALF following PFP exposure. LDH activity (A) and total protein (B) were measured in BALF. In general, LDH activity was below the detection limit (BDL) and indistinguishable from background in all neonates reared in FA. In contrast, adult rats had significantly higher basal levels of LDH. Following PFP exposure, an upward trend in neonates, with a significant increase in LDH activity observed 24 h post exposure. Interestingly, a transient drop of LDH activity was detected 2 h post PFP exposure in adult rats (A). Similar to LDH activity, total BALF protein was inherently higher in adult rats. While neonate levels remained unchanged following exposure, a significant increase in BALF protein levels were observed in adults 24 h post PFP exposure (B). After

against PCNA was evaluated in midlevel bronchiolar airways (Fig. 6). Protein abundance followed a similar trend compared with gene expression. Cell nuclear positive PCNA cells were abundant in 7-day postnatal rats reared in FA (Fig. 6A). PCNA abundance was reduced 2 hours following PFP exposure in 7-day animals, where staining became diffuse and strips of bronchiolar epithelia were observed to be devoid of nuclear PCNA (brackets, Fig. 6C). PCNA staining returned to steady state by 24 h post PFP exposure (Fig. 6E). In stark contrast, PCNA positive cells were rarely observed in FA adults (Fig. 6B). PFP exposure at either 2 or 24 h time points did not affect PCNA expression in adult animals (Figs. 6D and 6F).

DISCUSSION

In the current study, we found that exposure to an atmosphere containing a low dose of ultrafine particles elicits biological changes that greatly differ between young adult and neonatal rats. We focused our efforts on the conducting airways, due to the fact that extensive development of these airways occurs in the postnatal period and that exacerbation of many airway diseases, such as bronchitis and asthma have been linked to either acute or chronic exposures to PM in young children (Ciccone *et al.*, 1998; Brauer *et al.*, 2007; Morgenstern *et al.*, 2008). For this study, we assessed cytotoxicity, gene expression, and protein changes in an attempt to characterize differences between neonates and adults, which may explain the differential susceptibility between the ages.

We found that neonatal rats are more susceptible to PFP with significant increases in markers of cytotoxicity following exposure. Although the epithelial cytotoxic responses were mild, permeable cells were observed and significant increases in LDH activity in BALF were detected. Compared with adults, more macrophages incorporated ethidium homodimer-1, a marker of cytotoxicity in the neonatal lung. Our data agrees with the previous findings by Li *et al.* (2003) showing that ultrafine particles damage macrophages and cause formation of vacuoles in RAW 264.7 macrophages *in vitro*. Macrophages are also significantly affected by ultrafine particles in studies by Rouse *et al.* (2008), where particle-laden macrophages were noted after inhalation of butadiene soot. Furthermore, as a more global indicator of overall cell leakiness, LDH activity was found to be increased in the neonates but not in adults. This is also in agreement with our previous work using a diffusion soot particle, with a different EC/OC ratio and lower levels of attached PAH, where we showed significant LDH elevation in neonates 24 h after an acute lower-PAH containing diffusion flame exposure (Van Winkle *et al.*, 2010). In contrast to neonates, ethidium positive membrane permeable cells were rarely observed in adults, and LDH activity was not elevated after exposure. These results indicate that even at these low levels of exposure, neonates are more susceptible than adults.

We used a previously characterized premixed flame (PFP) generation system (Lee *et al.*, 2010) to expose neonatal and adult rats. Sprague-Dawley rats were chosen as the animal model because of their larger neonatal and adult sizes, compared with mice, and their use in previous PM studies (Roberts *et al.*, 2009; Van Winkle *et al.*, 2010; Zhong *et al.*, 2010). Animals were exposed to a single 6 h acute exposure to 22.4 $\mu g/m^3$ PFP. This dose was selected because it is below the 2006 EPA revised 24 h average $PM_{2.5}$ NAAQS of 35 $\mu g/m^3$ and approximates the measured levels of PM in this size range in downtown Fresno, CA. A fuel-rich flame environment generates carbonaceous soot in addition to a variety of allyl radicals, which further react to yield the formation of benzene (Marinov *et al.*, 1998). Benzene combined with additional radicals generates PAH (i.e., naphthalene, fluorenes, and phenanthrenes) (Castaldi *et al.*, 1996; Lindstedt, 1994), which we have characterized and quantified in our chambers. Although methylated biphenyls were the most abundant aromatic species in the vapor phase, the sum of mono, poly, and unsubstituted naphthalenes constituted the majority of the detected PAHs in the vapor and particulate phases. Furthermore, it is important to note that while two-ringed naphthalenes were the dominant species, three-ringed fluorene and phenanthrene, four-ringed pyrene, and five-ringed benzopyrenes were detected in subnanogram quantities.

We have previously shown that an acute *in vivo* exposure of a different type of PM, low PAH containing diffusion flame soot (DFP), elicits age-specific antioxidant and oxidative stress responses, discovering that young postnatal animals have increased susceptibility and respond uniquely to low PAH diffusion soot (Van Winkle *et al.*, 2010). A comparison of our results from the current study, with high PAH soot (PFP) is warranted. Previously, we have shown that gene expression is a sensitive marker for PM-induced oxidative stress and we have again applied antioxidant and oxidative stress RT-PCR arrays on microdissected conducting airways. Contrary to our expectations, the gene expression profile differed greatly in our PFP exposure compared with an acute diffusion flame exposure in both neonates and adults. Out of the 162 genes assessed, only 3 genes matched among the neonates, comparing across exposure types. Animals responded more robustly to PFP than to DFP, and both ages show a great number of genes altered within antioxidant and oxidative stress, necrosis and apoptosis, and proliferation and carcinogenesis categories. Comparing between ages, only 12 genes that were significantly altered by both PFP and DFP exposures matched between neonates and adults, a majority of these genes are for antioxidant enzymes.

←
normalizing LDH activity as a function of BALF protein, a more pronounced trend of increasing cell permeability was observed in neonates post PFP exposure (C). Data are plotted as means ± SEM ($n = 5$–17 rats/group, each rat was analyzed individually). BDL samples were treated as nondetects (NDs) and were imputed using the lnROS method. For the FA neonate group, NDs were replaced with the limit of detection where lnROS method was inapplicable. $p < 0.05$ are denoted as follows: * significantly different as compared with FA exposed 7-day postnatal controls, † significantly different from FA exposed adults, and ‡ significance compared against 2 h post PFP exposed neonates.

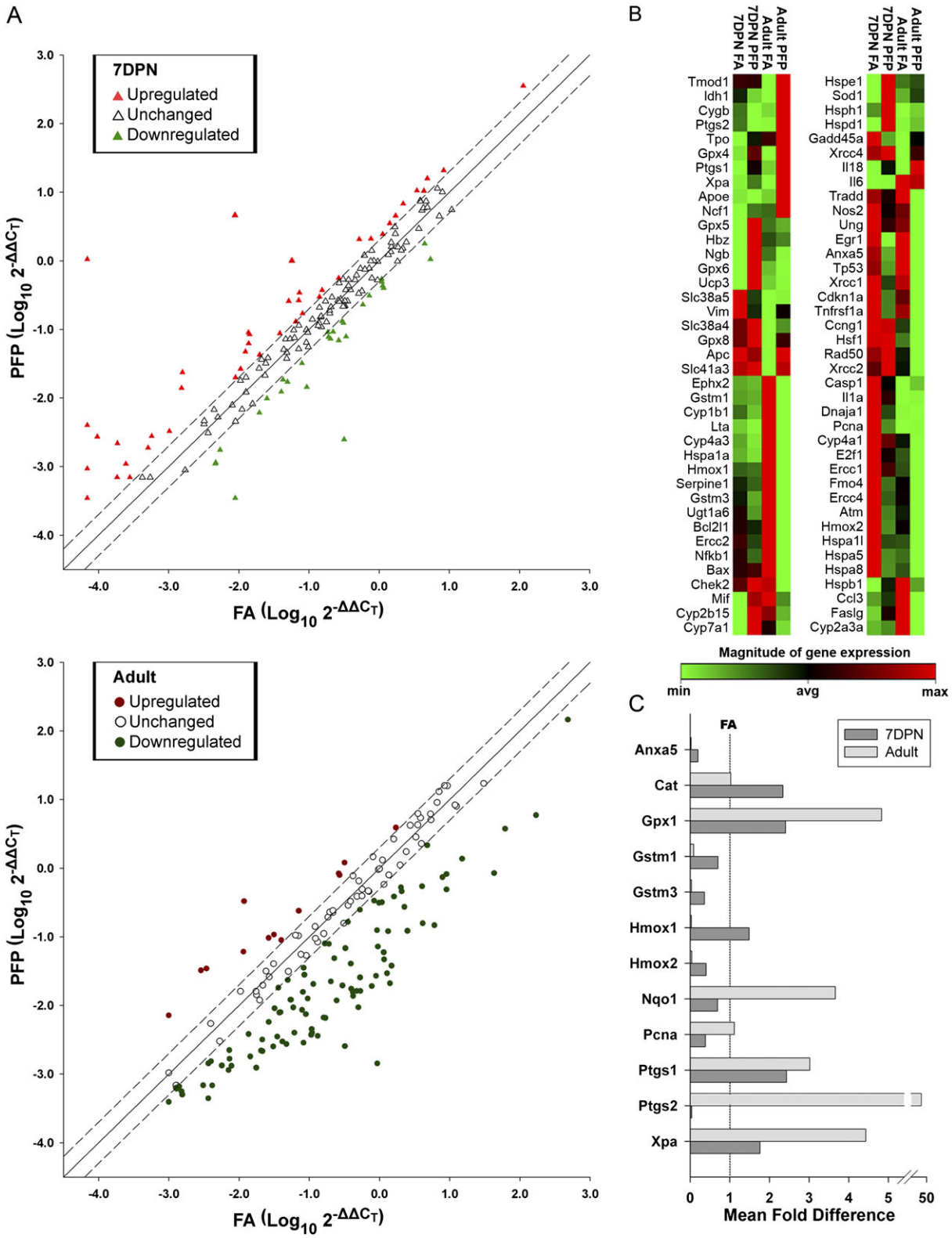

FIG. 5. Differentially expressed genes in microdissected airways. (A) Scatterplot of analyzed genes as a function of log of fold change plotted against exposures with FA on the x-axis and PFP on y-axis. The solid regression line indicates no exposure-induced change in the gene, and dashed lines are the 2 fold cutoff points. Genes expressed in neonates (top) are represented as triangles, where upregulated expression is colored pink, unchanged in white, and downregulated in lime. Gene expression in adults (bottom) are presented as circles, where upregulated genes are red, unchanged in white, and downregulated in green. Overall,

TABLE 3
PFP-Induced Gene Transcriptional Alterations in 7-Day Postnatal Rat Airways

Symbol	RefSeq	Gene Name	Fold Regulation	*p* Value
Antioxidant and oxidative stress				
Gpx1	NM_030826	Glutathione peroxidase 1	2.4084	0.017709
Gpx4	NM_017165	Glutathione peroxidase 4	2.6534	0.035767
Gpx5	XM_001059839	Glutathione peroxidase 5	58.0222	0.035673
Gpx6	NM_147165	Glutathione peroxidase 6	15249.42	0.018524
Gstm3	NM_031154	Glutathione S-transferase mu 3	−2.7707	0.025809
Hmox2	NM_024387	Heme oxygenase (decycling) 2	−2.4901	0.046847
Ptgs1	NM_017043	Prostaglandin-endoperoxide synthase 1	2.4303	0.023328
Ptgs2	NM_017232	Prostaglandin-endoperoxide synthase 2	−25.5822	0.025816
Tpo	NM_019353	Thyroid peroxidase	5.0122	0.036448
Ucp3	NM_013167	Uncoupling protein 3 (mitochondrial, proton carrier)	522.9152	0.031378
Xpa	XM_216403	Xeroderma pigmentosum, complementation group A	1.7608	0.008677
Heat shock proteins				
Hspa1l	NM_212546	Heat shock 70kD protein 1-like (mapped)	−3.2161	0.002062
Hspe1	NM_012966	Heat shock protein 1 (chaperonin 10)	3.1087	0.011288
Hspd1	NM_022229	Heat shock protein 1 (chaperonin)	3.0593	0.003225
Inflammation				
Lta	NM_080769	Lymphotoxin alpha (TNF superfamily, member 1)	−4.1394	0.003475
Necrosis and apoptosis				
Anxa5	NM_013132	Annexin A5	−5.0765	0.007664
Oxygen transporters				
Cygb	NM_130744	Cytoglobin	−6.4446	0.03966
Hbz	XM_213268	Hemoglobin, zeta	11.7297	0.007439
Ngb	NM_033359	Neuroglobin	9.1671	0.020161
Proliferation and carcinogenesis				
Ccnc	XM_342812	Cyclin C	2.1183	0.01864
Ccng1	NM_012923	Cyclin G1	2.1138	0.002406
Egr1	NM_012551	Early growth response 1	−126.776	0.002399
Tp53	NM_030989	Tumor protein p53	−4.2871	0.038778
Pcna	NM_022381	PCNA	−2.5916	0.048601

Since the gene expression pattern differed so markedly between our previous diffusion flame exposure (Van Winkle *et al.*, 2010) and the PFP exposure described in the current study, we hypothesized that the PAH content may play a large role in the cellular response to PM. Surprisingly, none of the xenobiotic metabolism genes responsible for solubilizing and metabolizing PAHs were significantly induced in the neonates. This may in part explain increased cytotoxicity; PAH containing particles have been shown to localize to lipids (Murphy *et al.*, 2008) through either chemical or biochemical processes. If a cell is unable to clear PAHs or induce enzymes to clear these PAHs, these compounds may persist in the cell and have the ability to enhance toxicity. Although the xenobiotic metabolizing cytochrome P450s could be detected by 7-day postnatal age, these neonates have immature xenobiotic metabolizing and detoxifying enzymes, which could further perturb their ability to clear PAHs (Cardoso *et al.*, 1993; Fanucchi, 2004; Ji *et al.*, 1994, 1995). In contrast to neonates, adult animals had significant increases in several cytochrome P450s (*CYP2A3a* and *CYP4A3*) and flavin-containing monooxygenases (*FMO2*, *FMO5*) genes following PFP exposure. Although we did not see significant increases in the expression of classical aryl hydrocarbon receptor (AhR) responsive genes (*CYP1A1*, *CYP1B1*) as Rouse *et al.* (2008) have reported, it has been shown that flavin-containing monooxygenase expression can be altered under the AhR-dependent pathway. Our results are in agreement with Celius *et al.* (2008), showing significant induction of *FMO2* and reduction of *FMO5* after AhR agonist TCDD treatment in liver.

←
neonates and adults have a divergent response. A trend showing upregulation was present in neonates (pink triangles), while adult animals were observed to have a substantial number of downregulated genes (green circles). (B) Heatmaps for all differentially expressed genes in airways of rats as a combination of age and/or exposure. All age and treatment groups were compared against FA exposed 7-day postnatal (7DPN) rats to elucidate age and exposure effects using HPRT as the reference gene. Genes that were differentially expressed at a p value less than 0.05 are shown ($n = 3$–6 rats/group). The relative magnitude of expression is indicated on a spectrum ranging from minimum (green) to maximum (red) detected. Expression patterns in 78 genes differed significantly as a combination of age and/or exposure effects. (C) The relative fold change compared with age-matched FA controls (line set at 1) for a subset of genes that were either significantly altered in 7-day-old postnatal and/or adult animals. Data are plotted as mean fold difference ± SEM ($n = 3$–6 rats/group, each rat was analyzed individually on the array).

TABLE 4
PFP-Induced Gene Transcriptional Alterations in Adult Rat Airways

Symbol	RefSeq	Gene Name	Fold Regulation	*p* Value
Antioxidant and oxidative stress				
Ctsb	NM_022597	Cathepsin B	3.0707	0.035618
Cygb	NM_130744	Cytoglobin	9.0559	0.014945
Duox2	NM_024141	Dual oxidase 2	70.0018	0.012265
Epx	XM_220834	Eosinophil peroxidase	7.6222	0.017935
Ephx2	NM_022936	Epoxide hydrolase 2, cytoplasmic	−36.9837	0.019421
Gpx1	NM_030826	Glutathione peroxidase 1	4.8268	0.036295
Gpx2	NM_183403	Glutathione peroxidase 2	6.9735	0.024608
Gpx6	NM_147165	Glutathione peroxidase 6	−191.402	0.044251
Gpx8	XM_215486	Glutathione peroxidase 8	4.2725	0.027142
Gsr	NM_053906	Glutathione reductase	−13.2797	0.028066
Gstm1	NM_017014	Glutathione S-transferase mu 1	−11.0965	0.001293
Gstm3	NM_031154	Glutathione S-transferase mu 3	−27.0246	0.013771
Hmox1	NM_012580	Heme oxygenase (decycling) 1	−30.9446	0.000458
Hmox2	NM_024387	Heme oxygenase (decycling) 2	−24.3281	0.028834
Idh1	NM_031510	Isocitrate dehydrogenase 1 (NADP+), soluble	5.6885	0.015345
Nox4	NM_053524	NADPH oxidase 4	3.5661	0.038669
Por	NM_031576	P450 (cytochrome) oxidoreductase	−7.477	0.009219
Prdx1	NM_057114	Peroxiredoxin 1	3.882	0.013839
Prdx3	NM_022540	Peroxiredoxin 3	3.0562	0.048917
Prnp	NM_012631	Prion protein	7.9351	0.031433
Ptgs2	NM_017232	Prostaglandin-endoperoxide synthase 2	49.6539	0.023834
Slc41a3	NM_001037492	Solute carrier family 41, member 3	5.2298	0.047979
Sod1	NM_017050	Superoxide dismutase 1, soluble	3.6862	0.031726
Sod2	NM_017051	Superoxide dismutase 2, mitochondrial	3.5975	0.041264
Xpa	XM_216403	Xeroderma pigmentosum, complementation group A	4.4286	0.010963
Heat shock proteins				
Hspa4	NM_153629	Heat shock protein 4	1.8433	0.016881
Hspa1a	NM_031971	Heat shock 70kD protein 1A	−67.6156	0.014389
Inflammation				
Ccl21b	NM_001008513	Chemokine (C-C motif) ligand 21b (serine)	−11.0321	0.016656
Ccl3	NM_013025	Chemokine (C-C motif) ligand 3	−7.5797	0.046574
Il18	NM_019165	Interleukin 18	3.3456	0.002379
Lta	NM_080769	Lymphotoxin alpha (TNF superfamily, member 1)	−12.2652	0.010425
Nfkb1	XM_342346	Nuclear factor of kappa light polypeptide gene enhancer in B-cells 1	−33.0979	0.01622
Necrosis and apoptosis				
Anxa5	NM_013132	Annexin A5	−41.4567	0.012066
Bax	NM_017059	Bcl2-associated X protein	−33.2827	0.010506
Bcl2l1	NM_031535	Bcl2-like 1	−40.9219	0.025367
Chek2	NM_053677	CHK2 checkpoint homolog (*Schizosaccharomyces. pombe*)	−15.4004	0.013171
Ercc2	XM_218424	Excision repair cross-complementing rodent repair deficiency, complementation group 2	−27.6876	0.010995
Ercc4	XM_222534	Excision repair cross-complementing rodent repair deficiency, complementation group 4	−14.0267	0.026123
Rad23a	NM_001013190	RAD23 homolog A (*Saccharomyces. cerevisiae*)	−7.4534	0.03773
Tradd	XM_341671	TNFRSF1A-associated via death domain	−26.2046	0.030071
Tnfrsf1a	NM_013091	Tumor necrosis factor receptor superfamily, member 1a	−53.5655	0.046099
Ugt1a6	NM_057105	UDP glucuronosyltransferase 1 family, polypeptide A6	−15.3658	0.010749
Ung	NM_001013124	Uracil-DNA glycosylase	−24.0967	0.030458
Xrcc1	NM_053435	X-ray repair complementing defective repair in Chinese hamster cells 1	−29.3218	0.005521
Proliferation and carcinogenesis				
Ccnd1	NM_171992	Cyclin D1	−3.9014	0.008242
Egr1	NM_012551	Early growth response 1	−127.066	0.002162
Cdkn1a	NM_080782	Cyclin-dependent kinase inhibitor 1A (p21, Cip1)	−20.8561	0.016276
Igfbp6	NM_013104	Insulin-like growth factor binding protein 6	−43.9	0.019266
Tp53	NM_030989	Tumor protein p53	−22.9176	0.026688
Xenobiotic metabolism				
Cyp2a3a	NM_012542	Cytochrome P450, family 2, subfamily A, polypeptide 3a	−10.7957	0.001177
Cyp4a3	NM_175760	Cytochrome P450, family 4, subfamily a, polypeptide 3	−9.4802	0.005024
Fmo2	NM_144737	Flavin containing monooxygenase 2	5.8038	0.026673
Fmo5	NM_144739	Flavin containing monooxygenase 5	−9.1731	0.023699

We examined gene expression changes at a single time point (24 h) after exposure. This time point was selected to compare with previous results obtained from our diffusion flame inhalation study (Van Winkle *et al*., 2010). However, it is very likely that the temporal patterns of the antioxidant, proliferation, and xenobiotic metabolizing genes differ by age and exposure. This could explain differences in expression of several antioxidant genes between the diffusion flame soot exposure (Van Winkle *et al*., 2010), the butadiene soot exposures (Rouse *et al*., 2008), and the PFP reported here. Another possible explanation is the differences in PAH composition of these atmospheres. Butadiene soot contains large planar PAHs-like pyrenes and benzo(a)pyrenes (Penn *et al*., 2005). This is in contrast to the diffusion flame soot we used previously which contains a mixture of pyrene, quinoline, and naphthalene (Van Winkle *et al*., 2010) and our ethylene generated PFP, reported in this study, which consists essentially of smaller PAHs-like biphenyls and substituted naphthalenes. While much previous work has been done regarding metabolism and toxicity of naphthalene, it has been shown that generally, neither inhalation nor intraperitoneal injections of naphthalene result in lung toxicity in rats and it is mainly a mouse-specific lung toxicant (Buckpitt *et al*., 2002; Lin *et al*., 2009; Van Winkle *et al*., 1999; West *et al*., 2001). It is surprising then that even though naphthalene is the most abundant PAH found in the PFP particulate phase, we were able to observe the presence of cytotoxic cells. We postulate that toxicity may partly be due to the presence of lower abundance aryl hydrocarbon receptor (AhR) agonistic PAHs (i.e., pyrenes, benzopyrenes, and anthanthrenes) present in subnanogram per cubic meter quantities in the PFP atmosphere.

While both neonatal and adult rats were exposed to the same atmospheric PFP concentration in the exposure chambers, a multitude of factors may have affected dose delivered in the neonates versus adults. Neonatal rats have higher ventilation and oxygen consumption rates than adult rats normalized to body weight (Mortola, 1991). Differences in breathing frequency, body size, and mean airway diameter change deposition patterns, which may increase dose in the neonates compared with the adults. Alternatively, because the pups were exposed with their dams in the exposure chambers, the delivered dose to the neonate may have been reduced due to huddling under the dam. These two factors potentially offset each other but it is not possible to know to what degree. For a 6-h exposure, we chose to expose the neonates with their dam to minimize the effects of stress, heat loss, and nutritional changes. This exposure strategy has been used for other inhalation studies (Clerch and Massaro, 1992; Joad *et al*., 1995), but it is important to keep these limitations in mind in terms of delivered dose.

Even after a single acute exposure to PFP, cell cycle checkpoint cyclins and *Tp53* were significantly changed in both ages. It is reasonable, because PAH-rich particles, like diesel exhaust, in the presence of cytochrome P450 reductase, have been shown to generate reactive oxygen species that damage DNA and induce strand breaks (Kumagai *et al*., 1997). We questioned the implications of PFP exposure on continuing lung growth and development and analyzed the protein: PCNA, a marker of cell proliferation. As expected, basal expression of PCNA was significantly higher in the developing neonates. However, we found significant decreases in both protein expression at 2 h and gene expression at 24 h post exposure in the neonates. In contrast, we have previously reported that neither PCNA gene nor protein expression were significantly altered in neonates and adults following an acute low PAH containing diffusion flame exposure (Van Winkle *et al*., 2010). Our gene expression results are in agreement with Lee *et al*. (2010), who also found reduced PCNA expression in neonates 24 h after PFP soot exposure, our RT^2 Profiler PCR Array confirms these previous results obtained with conventional qRT-PCR. In addition, we show focal patches of PCNA-deficient cells in the current study that are detected at 2-h post exposure. This builds upon the evidence that proliferative

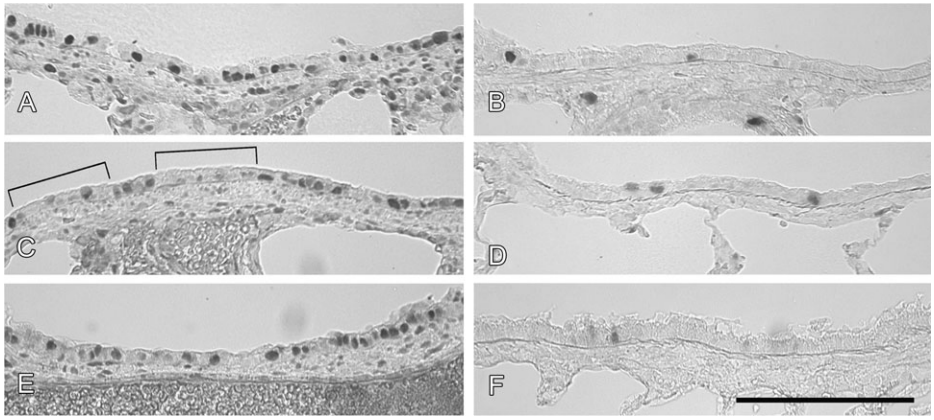

FIG. 6. Immunohistochemical staining of PCNA in the airways of 7-day postnatal (A, C, and E) and adult (B, D, and F) exposed to either FA (A, B) or PFP, examined two (C, D) or 24 h (E, F) after cessation of exposure. Basally, 7-day old neonates exposed to FA had abundant cells with nuclear staining for PCNA (A). In contrast, PCNA was scarce in FA exposed adults (B). Following 2 hours post PFP exposure, PCNA in 7-day neonates became diffuse, and strips of epithelium were observed to be devoid of nuclear PCNA staining (brackets) (C). PCNA staining returned to steady state by 24 h post PFP exposure (E). PCNA was unaffected after PFP exposure in adult rats (D and F). Scale bar for A–F (shown in F) is 50 μm.

capabilities of neonates, but not adults, are impaired by PFP. We postulate that the decrease in PCNA expression is a rapid and early response to PFP exposure that persists for at least 24 h. PFP has previously been shown to cause significant reductions in bronchiolar diameter and length in developing rats after a 3-week subchronic exposure (Lee *et al.*, 2010). Altered proliferation patterns during development could be a contributing factor to these gross changes in airway architecture and may result in reduced lung function. Additionally, since we were able to observe similar results across two separate studies and saw changes in numerous genes involved in the proliferative response pathways, this supports that we have a reproducible exposure and biologic effect, a necessary prerequisite to perform repeatable biologic experiments to be able to tease apart the mechanisms of PM susceptibility.

We postulate that developing neonates have a limited ability to deviate from the normal developmental pattern and this inability to respond to ultrafine particulates enhances oxidative stress, causes cellular injury, and perturbs normal airway development. Similar outcomes using two different particle generation systems as well as the same exposure system used for two different time points validates our results and underscores the usefulness and necessity of having defined exposure conditions that can be replicated for additional in depth studies of biologic mechanisms of altered growth and antioxidant responses. Future time course studies of the intracellular signaling cascades that regulate these processes will be required to determine whether the entire temporal pattern between neonates and adults differ in response to PM and will allow us to begin to address the mechanisms for elevated susceptibility in neonatal animals.

This study shows that a short-term low-dose inhalation exposure to combustion derived ultrafine particles induces markers of cytotoxicity and alters gene and protein expression patterns in the conducting airways of developing neonates compared with adults. Our data strongly suggests that adult animals are an inappropriate model for evaluating responses to PM in susceptible populations, such as young children. Based on our results, neonates have a unique "inability" to respond to environmental exposures by changing gene expression compared with adults. Compared with adult animals, developing neonates are more susceptible to PAH-rich ultrafine PM, exhibiting increased cellular toxicity in the lung affecting airway proliferation patterns, which may result in the perturbation of normal lung development.

SUPPLEMENTARY DATA

Supplementary data are available online at http://toxsci.oxfordjournals.org/.

FUNDING

Support for the University of California at Davis core facilities used in this work: the Cellular and Molecular Imaging Core Facility (ES005707) and the inhalation exposure facility at the California National Primate Research Center (RR00169). Although the research described in the article has been funded primarily by the United States Environmental Protection Agency through grant RD-83241401-0 to the University of California, Davis, it has not been subject to the agency's required peer and policy review and, therefore, does not necessarily reflect the views of the agency and no official endorsement should be inferred. The project described was also supported in part by Award Number P42ES004699 from the National Institute of Environmental Health Sciences. Mr Chan's effort was supported by a training program in Environmental Health Sciences (T32 ES007058-33) funded by the National Institute of Environmental Health Sciences.

CONFLICT OF INTEREST

Dr Laura Van Winkle has identified a potential competing financial interest with the American Petroleum Institute (API). Dr Van Winkle is a co-investigator on a research grant from API to study the kinetics of naphthalene bioactivation in the lung and has received honoraria from API for speaking at research conferences sponsored by API on naphthalene. API did not fund any of the work presented in the attached study and the research grant funded by API has complete freedom to publish the results regardless of whether they are in API's interest, and without input from API, in keeping with University of California policy. The remaining authors declare they have no actual or potential competing financial interests.

ACKNOWLEDGMENTS

We are grateful to the following people for their skilled technical assistance during exposures, sample collection, and processing: Brian Tarkington, Ashley Cooper, Louise Olson, Patricia Edwards, Trenton Combs, and Judy Shimizu. We acknowledge Michael Kleeman's laboratory at UC Davis for EC/OC sample analysis and Barbara Zielinska at the DRI for filter and vapor phase PAH speciation. Finally, we thank Jessie Charrier, Cris Grodzki, Matt Herring, and Keisha Williams for reading and editing the manuscript. The content is solely the responsibility of the authors and does not necessarily represent the official views of the National Institute of Environmental Health Sciences or the National Institutes of Health.

REFERENCES

ALA. (2009). *American Lung Association State of the Air: 2009*. American Lung Association, New York, NY.

Baker, G. L., Shultz, M. A., Fanucchi, M. V., Morin, D. M., Buckpitt, A. R., and Plopper, C. G. (2004). Assessing gene expression in lung subcompartments utilizing in situ RNA preservation. *Toxicol. Sci.* **77,** 135–141.

Bearer, C. F. (1995). How are children different from adults. *Environ. Health Perspect.* **103,** 7–12.

Branis, M., Safranek, J., and Hytychova, A. (2009). Exposure of children to airborne particulate matter of different size fractions during indoor physical education at school. *Build. Environ.* **44,** 1246–1252.

Brauer, M., Hoek, G., Smit, H. A., de Jongste, J. C., Gerritsen, J., Postma, D. S., Kerkhof, M., and Brunekreef, B. (2007). Air pollution and development of asthma, allergy and infections in a birth cohort. *Eur. Respir. J.* **29,** 879–888.

Buckpitt, A., Boland, B., Isbell, M., Morin, D., Shultz, M., Baldwin, R., Chan, K., Karlsson, A., Lin, C., Taff, A., *et al.* (2002). Naphthalene-induced respiratory tract toxicity: Metabolic mechanisms of toxicity. *Drug Metab. Rev.* **34,** 791–820.

Cardoso, W. V., Stewart, L. G., Pinkerton, K. E., Ji, C., Hook, G. E., Singh, G., Katyal, S. L., Thurlbeck, W. M., and Plopper, C. G. (1993). Secretory product expression during Clara cell differentiation in the rabbit and rat. *Am. J. Physiol.* **264,** L543–L552.

Castaldi, M. J., Marinov, N. M., Melius, C. F., Huang, J., Sekan, S. M., Pitz, W. J., and Westbrook, C. K. (1996). Experimental and modeling investigation of aromatic and polycyclic aromatic hydrocarbon formation in a premixed ethylene flame. *Symposium (International) on Combustion* **26,** 693–702.

Celius, T., Roblin, S., Harper, P. A., Matthews, J., Boutros, P. C., Pohjanvirta, R., and Okey, A. B. (2008). Aryl hydrocarbon receptor-dependent induction of flavin-containing monooxygenase mRNAs in mouse liver. *Drug Metab. Dispos.* **36,** 2499–2505.

Chomczynski, P., and Sacchi, N. (1987). Single-step method of RNA isolation by acid guanidinium thiocyanate-phenol-chloroform extraction. *Anal. Biochem.* **162,** 156–159.

Ciccone, G., Forastiere, F., Agabiti, N., Biggeri, A., Bisanti, L., Chellini, E., Corbo, G., Dell'Orco, V., Dalmasso, P., Volante, T. F., *et al.* (1998). Road traffic and adverse respiratory effects in children. SIDRIA Collaborative Group. *Occup. Environ. Med.* **55,** 771–778.

Clerch, L. B., and Massaro, D. (1992). Rat lung antioxidant enzymes: Differences in perinatal gene expression and regulation. *Am. J. Physiol.* **263,** L466–L470.

Dockery, D. W. (2009). Health effects of particulate air pollution. *Ann. Epidemiol.* **19,** 257–263.

Fanucchi, M. (2004). In *Development of Antioxidant and Xenobiotic Metabolizing Enzyme Systems*. Elsevier, San Diego, CA.

Hammond, T. G., and Mobbs, M. (1984). Lung oedema—microscopic detection. *J. Appl. Toxicol.* **4,** 219–221.

Helsel, D. R. (2005). More than obvious: Better methods for interpreting nondetect data. *Environ. Sci. Technol.* **39,** 419a–423a.

Herner, J. D., Aw, J., Gao, O., Chang, D. P., and Kleeman, M. J. (2005). Size and composition distribution of airborne particulate matter in Northern California: I–Particulate mass, carbon, and water-soluble Ions. *J. Air Waste Manag. Assoc.* **55,** 30–51.

Hinners, R., Burkart, J., and Punte, C. (1968). Animal inhalation exposure chambers. *Arch. Environ. Health.* **16,** 194–206.

Ibald-Mulli, A., Wichmann, H. E., Kreyling, W., and Peters, A. (2002). Epidemiological evidence on health effects of ultrafine particles. *J. Aerosol. Med.* **15,** 189–201.

Ji, C. M., Cardoso, W. V., Gebremichael, A., Philpot, R. M., Buckpitt, A. R., Plopper, C. G., and Pinkerton, K. E. (1995). Pulmonary cytochrome P-450 monooxygenase system and Clara cell differentiation in rats. *Am. J. Physiol.* **269,** L394–L402.

Ji, C. M., Plopper, C. G., Witschi, H. P., and Pinkerton, K. E. (1994). Exposure to sidestream cigarette smoke alters bronchiolar epithelial cell differentiation in the postnatal rat lung. *Am. J. Respir. Cell. Mol. Biol.* **11,** 312–320.

Joad, J. P., Ji, C., Kott, K. S., Bric, J. M., and Pinkerton, K. E. (1995). In utero and postnatal effects of sidestream cigarette smoke exposure on lung function, hyperresponsiveness, and neuroendocrine cells in rats. *Toxicol. Appl. Pharmacol.* **132,** 63–71.

Karnovsky, M. J. (1965). A formaldehyde-glutaraldehyde fixative of high osmolality for use in electron microscopy. *J. Cell Biol.* **27,** 137A–138A.

Kumagai, Y., Arimoto, T., Shinyashiki, M., Shimojo, N., Nakai, Y., Yoshikawa, T., and Sagai, M. (1997). Generation of reactive oxygen species during interaction of diesel exhaust particle components with NADPH-cytochrome P450 reductase and involvement of the bioactivation in the DNA damage. *Free Radic. Biol. Med.* **22,** 479–487.

Langston, C. (1983). Normal and abnormal structural development of the human lung. *Prog. Clin. Biol. Res.* **140,** 75–91.

Lee, D., Wallis, C., Wexler, A. S., Schelegle, E. S., Van Winkle, L. S., Plopper, C. G., Fanucchi, M. V., Kumfer, B., Kennedy, I. M., *et al.* (2010). Small particles disrupt postnatal airway development. *J. Appl. Physiol.* **109,** 1115–1124.

Li, N., Sioutas, C., Cho, A., Schmitz, D., Misra, C., Sempf, J., Wang, M., Oberley, T., Froines, J., and Nel, A. (2003). Ultrafine particulate pollutants induce oxidative stress and mitochondrial damage. *Environ. Health Perspect.* **111,** 455–460.

Lin, C. Y., Wheelock, A. M., Morin, D., Baldwin, R. M., Lee, M. G., Taff, A., Plopper, C., Buckpitt, A., and Rohde, A. (2009). Toxicity and metabolism of methylnaphthalenes: Comparison with naphthalene and 1-nitronaphthalene. *Toxicology* **260,** 16–27.

Lindstedt, R. P. (1994). Formation and destruction of aromatic-compounds and soot in flames. *Abstr. Pap. Am. Chem. Soc.* **207,** 22–FUEL.

Marinov, N. M., Pitz, W. J., Westbrook, C. K., Vincitore, A. M., Castaldi, M. J., Senkan, S. M., and Melius, C. F. (1998). Aromatic and polycyclic aromatic hydrocarbon formation in a laminar premixed n-butane flame. *Combust. Flame* **114,** 192–213.

Mills, N. L., Donaldson, K., Hadoke, P. W., Boon, N. A., MacNee, W., Cassee, F. R., Sandstrom, T., Blomberg, A., and Newby, D. E. (2009). Adverse cardiovascular effects of air pollution. *Nat. Clin. Pract. Cardiovasc. Med.* **6,** 36–44.

Morgenstern, V., Zutavern, A., Cyrys, J., Brockow, I., Koletzko, S., Kramer, U., Behrendt, H., Herbarth, O., von Berg, A., Bauer, C. P., *et al.* (2008). Atopic diseases, allergic sensitization, and exposure to traffic-related air pollution in children. *Am. J. Respir. Crit. Care Med.* **177,** 1331–1337.

Morrow, P. E., and Mercer, T. T. (1964). A Point-to-Plane electrostatic precipitator for particle size sampling. *AIHAJ* **25,** 8–14.

Mortola, J. P. (1991). Hamsters versus rats: Ventilatory responses in adults and newborns. *Respir. Physiol.* **85,** 305–317.

Murphy, G., Jr.., Rouse, R. L., Polk, W. W., Henk, W. G., Barker, S. A., Boudreaux, M. J., Floyd, Z. E., and Penn, A. L. (2008). Combustion-derived hydrocarbons localize to lipid droplets in respiratory cells. *Am. J. Respir. Cell. Mol. Biol.* **38,** 532–540.

Norris, G., YoungPong, S. N., Koenig, J. Q., Larson, T. V., Sheppard, L., and Stout, J. W. (1999). An association between fine particles and asthma emergency department visits for children in Seattle. *Environ. Health Perspect.* **107,** 489–493.

Pekkanen, J., Timonen, K. L., Ruuskanen, J., Reponen, A., and Mirme, A. (1997). Effects of ultrafine and fine particles in urban air on peak expiratory flow among children with asthmatic symptoms. *Environ. Res.* **74,** 24–33.

Penn, A., Murphy, G., Barker, S., Henk, W., and Penn, L. (2005). Combustion-derived ultrafine particles transport organic toxicants to target respiratory cells. *Environ. Health Perspect.* **113,** 956–963.

Peters, A., Dockery, D. W., Heinrich, J., and Wichmann, H. E. (1997). Short-term effects of particulate air pollution on respiratory morbidity in asthmatic children. *Eur. Respir. J.* **10,** 872–879.

Pey, J., Querol, X., Alastuey, A., Rodriguez, S., Putaud, J. P., and Van Dingenen, R. (2009). Source apportionment of urban fine and ultra-fine particle number concentration in a Western Mediterranean city. *Atmos. Environ.* **43,** 4407–4415.

Robert, M. A., VanBergen, S., Kleeman, M. J., and Jakober, C. A. (2007). Size and composition distributions of particulate matter emissions: Part 1—light-duty gasoline vehicles. *J. Air. Waste Manag. Assoc.* **57,** 1414–1428.

Roberts, J. R., Young, S. H., Castranova, V., and Antonini, J. M. (2009). The soluble nickel component of residual oil fly ash alters pulmonary host defense in rats. *J. Immunotoxicol.* **6,** 49–61.

Rouse, R. L., Murphy, G., Boudreaux, M. J., Paulsen, D. B., and Penn, A. L. (2008). Soot nanoparticles promote biotransformation, oxidative stress, and inflammation in murine lungs. *Am. J. Respir. Cell. Mol. Biol.* **39,** 198–207.

Shumway, R. H., Azari, R. S., and Kayhanian, M. (2002). Statistical approaches to estimating mean water quality concentrations with detection limits. *Environ. Sci. Technol.* **36,** 3345–3353.

USEPA. (2009). *U.S. EPA Green Book—Particulate Matter (PM-2.5) Nonattainment Areas (1997 Standard).* U.S Environmental Protection Agency, Research Triangle Park, NC.

Van Winkle, L. S., Chan, J. K., Anderson, D. S., Kumfer, B. M., Kennedy, I. M., Wexler, A. S., Wallis, C., Abid, A. D., Sutherland, K. M., *et al.* (2010). Age specific responses to acute inhalation of diffusion flame soot particles: Cellular injury and the airway antioxidant response. *Inhal. Toxicol.* **22**(Suppl 2), 70–83.

Van Winkle, L. S., Isaac, J. M., and Plopper, C. G. (1996). Repair of naphthalene-injured microdissected airways in vitro. *Am. J. Respir. Cell. Mol. Biol.* **15,** 1–8.

Van Winkle, L. S., Johnson, Z. A., Nishio, S. J., Brown, C. D., and Plopper, C. G. (1999). Early events in naphthalene-induced acute Clara cell toxicity: Comparison of membrane permeability and ultrastructure. *Am. J. Respir. Cell. Mol. Biol.* **21,** 44–53.

West, J. A., Pakehham, G., Morin, D., Fleschner, C. A., Buckpitt, A. R., and Plopper, C. G. (2001). Inhaled naphthalene causes dose dependent Clara cell cytotoxicity in mice but not in rats. *Toxicol. Appl. Pharmacol.* **173,** 114–119.

Wilson, H. H., Chauhan, J., Kerry, P. J., and Evans, J. G. (2001). Ethanol vapour-fixation of rat lung for immunocytochemistry investigations. *J. Immunol. Methods* **247,** 187–190.

Zhong, C. Y., Zhou, Y. M., Smith, K. R., Kennedy, I. M., Chen, C. Y., Aust, A. E., and Pinkerton, K. E. (2010). Oxidative injury in the lungs of neonatal rats following short-term exposure to ultrafine iron and soot particles. *J. Toxicol. Environ. Health A* **73,** 837–847.